CONSTRUCTING A LOW-COST ELF/VLF REMOTE SENSING TO OBSERVE TWEEK SFERICS GENERATED BY LIGHTNING DISCHARGES

Le MINH TAN[1], Marjan MARBOUTI[2] and Keyvan GHANBARI[2]
[1]*Department of Physics, Faculty of Natural Science and Technology, Tay Nguyen University*
567 Le Duan Street, Buon Ma Thuot City, DakLak Province, 630000, Vietnam, +84935318151, Email: lmtan@ttn.edu.vn
[2]*Energy Engineering and Physics Department, Amirkabir university of technology, 15875-4413, Tehran, Iran*

Abstract: The Extremely Low Frequency (ELF) and Very Low frequency (VLF) technique are useful for studying the lower ionosphere of the Earth. Exploring this region has been begun in Viet Nam. We constructed the ELF/VLF remote sensing with low cost. This system includes a loop antenna, a pre-amplifier, a sound card, a PC with software and a GPS receiver. After surveying its characteristics, we found that the antenna has the high sensitivity and the pre-amplifier designed has the flat frequency response with frequency from 1 kHz to 20 kHz. It can record sferics generated by lightning discharges to estimate the parameters of the nighttime D-region ionosphere. It is also a teaching module to educate students in Space physics.

Keywords: *ELF/VLF remote sensing, normalized antenna sensitivity, frequency response, tweek sferics, D-region ionosphere.*

I. INTRODUCTION

The height of the D layer, the lowest layer of the Earth' ionosphere, is from 60 – 75 km in the day and 75 – 95 km in the night [1]. The Extremely Low Frequency (ELF, 3 – 3000 Hz) and Very Low Frequency (VLF, 3 – 30 kHz) technique is powerful for exploring the physical processes of the D layer. The ELF/VLF pulses radiated by lightning discharges are recorded at the receivers through the propagation in the Earth - Ionosphere waveguide (EIWG). They can also propagate in the magnetosphere to the other hemisphere [2]. The sferics commonly consist of VLF impulse lasting less than 1 ms and ELF component extending about 1-3 ms [3]. These electromagnetic pulses can spread very far away tens of thousands of kilometers with cut-off frequency of 1.8 kHz [4]. Sometimes, the "hooks" occur on the spectrogram, which are called “tweeks” or “tweek atmospherics” and heard as chirping [5]. Tweek method has been used to calculate the propagation distance from lightning discharges to the receivers, reflection height and electron density of the D layer [6 - 9].

Currently, there are many ELF/VLF receivers made by the different ways. However, these devices have been focused only some simple parts, and their factors affecting the characteristics of operation have not thoroughly been analyzed…Many researchers have designed the receivers to record the narrowband VLF signals for daytime ionosphere monitoring [10-12]. Furthermore, there is a lack of equipments for observing nighttime D-layer ionosphere and for teaching Space physics and Atmospheric physics objects at our university. Therefore, construction of ELF/VLF remote sensing becomes necessary.

In this paper, we aim to present how to design the basic system of ELF/VLF remote sensing, evaluate its main characteristics and illustrate the ability of the recording data of this monitor.

II. SYSTEM DESIGN

The ELF/VLF remote sensing consists of main parts: a loop antenna, a pre-amplifier, Data Acquisition (ADC (Analog to Digital Converter), PC and SpectrumLab) and GPS receiver (Figure 1).

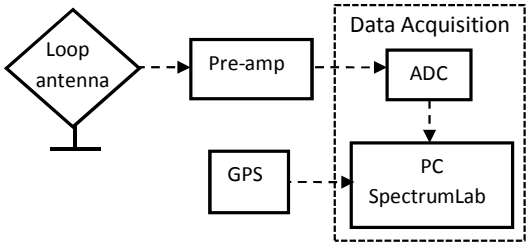

Figure 1. Block diagram of ELF/VLF remote sensing system

2.1. Antenna Design

The magnetic antenna is the loop with many turns of copper wire. Its shape is a square with the base of 1 m. The wire is chosen with the type of the 18 AWG (American Wire Gause). Figure 2 shows the shape of ELF/VLF antenna. The loop DC resistance (R_a), inductance (L_a), normalized antenna sensitivity (S_o), and the antenna turnover frequency (f_a) are calculated by following equations, respectively [13]:

$$R_a = 2.195\times10^{-8} N c_1 \sqrt{A} / d^2 \quad (1)$$

Manuscript received February 1, 2015; revised June 3, 2015

$$L_a = 2.00\times10^{-7} N^2 c_1 \sqrt{A}\left[\ln\left(\frac{c_1\sqrt{A}}{\sqrt{N}d}\right) - c_2\right] \quad (2)$$

$$S_o = 6.05\times10^{-3}\frac{\sqrt{R_a}}{NA} \quad (3)$$

$$f_a = \frac{R_a}{2\pi L_a} \quad (4)$$

Where, N is the number of turns, A is the area of the loop antenna (in m^2), d is the diameter of wire (in m). The f_a is the frequency where the inductive reactance and resistance reach the same value. With the square antenna, we choose $c_1 = 4$ and $c_2 = 1.217$ [14].

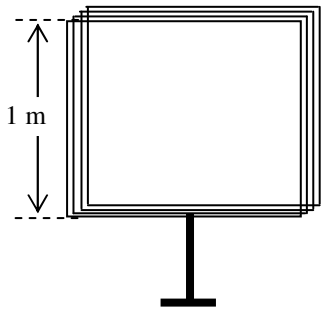

Figure 2. ELF/VLF antenna

Using equations (1), (2) for the copper wires with N = 14, A = 1 m^2, and $d = 1.02.10^{-3}$ m, we obtain $R_a \approx 1.2\ \Omega$ and $L_a \approx$ 0.9 mH. We use the instrument to measure those parameters. The resistance and inductance of the antenna are approximately1.24 Ω and 0.862 mH, respectively. Comparing with theoretical calculation, the relative errors are found by 4.4 % for resistance and 4.1 % for inductance. Using equation (4), we get f_a = 229 Hz. Under this frequency the loop resistance prevails over the inductive reactance, and we have a 6dB/octave roll off in the output signal. The normalized sensitivity of this antenna is 4.81 x 10^{-4} V/Hz$^{-1/2}$m^{-1}. This value is smaller than the value of the normalized sensitivity (S_o = 8,96 x 10^{-4} V/Hz$^{-1/2}$m^{-1}) of Paschal's antenna with the base of 0.567 m and 21 turns of 18 AWG wire [13]. It means that our loop is more sensitive than that reported by this author.

We use a silver shield to wrap the loop antenna and make the equipotential grounding to the metal box of the pre-amplifier. The antenna is installed at the quiet site. This reduces the noise caused by the AC sources and by high-frequency resonance due to the nearby radio broadcasting station.

2.2. Pre-amplifier design

The pre-amplifier designed has two stages. In Figure 3, the first stage of the pre-amplifier has the operational amplifier (Op-Amp) LT1028 which is an Op-Amp with the very low noise of 1.2 nV/$\sqrt{Hz}$ at 1kHz. Its noise is smaller than that of other Op-Amps such as TL081 (18 nV/$\sqrt{Hz}$), OP28 (3 nV/$\sqrt{Hz}$), and μA741 (90 nV/$\sqrt{Hz}$), etc. The input impedance of pre-amplifier is matched to the low impedance of the antenna. This leads the output voltage to be independent of frequency over a limited range. For that purpose, we use audio transformers TR1 (A262A1E) and build the turns ratio of 1:m (m = 12.6). This stage also is the low pass filter which contains an RC cell (R3 and C3). The cut-off frequency, f_{CL}, is obtained, f_{CL} = 33.9 kHz. At f = 20 Hz, we get the $R_{in} \approx 159\ \Omega$ ($R_{in} = 1/2\pi fC_1$). Therefore, we have $R_{in}/m^2 \approx 1 < R_a$. This condition is required for flat frequency response [13].

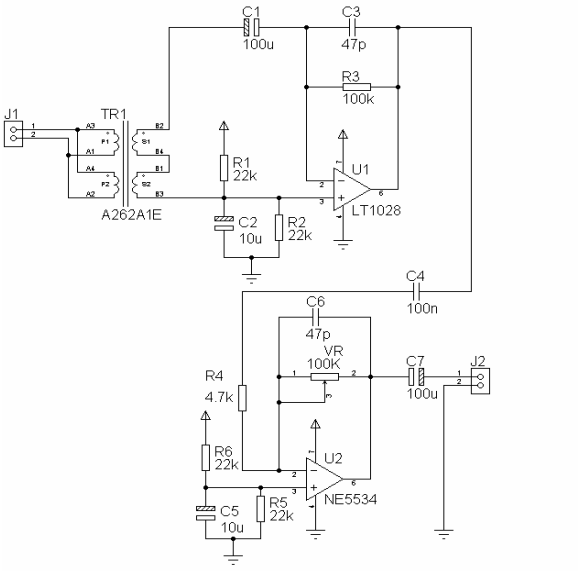

Figure 3. The circuit diagram of the pre-amplifier.

The second stage has a low-pass filter which contains an RC cell (VR and C6) and a high-pass filter with C4 and R4 (C4 = 100 nF, R4 = 4.7 kΩ). The function of VR is the negative feedback of Op-Amp (NE5534). The cut-off frequency is obtained f_{CH} = 339 Hz. This filter can reduce the hum noise generated by power lines. A single supply is used for the Op-Amps, hence they are biased the no-converting input by building a voltage divider with R1, R2, R5 and R6 [15]. The capacitors C2 and C5 bypass the voltage divider to attenuate resistor noise. To provide power to the pre-amplifier, we use a DC power supply which can adjust the output voltages.

The circuit layout is designed by using Altium software, and then the printed circuit board is also made. Figure 4a shows the printed circuit board. Figure 4b shows the printed circuit board assembled with the electronic components is enclosed in a metal box.

The ELF/VLF signals from the pre-amplifier are transferred to the computer via a RX-59 coaxial cable length of 150m. The audio transformer 1:1 is used to isolate ground of pre-amplifier and ground of the computer. The audio signals from the transformer go into the sound card on board of a PC (Realtek HD Audio). The ADC of sound card digitizes the output signal to transfer to the PC. The sampling frequency of the ADC is calibrated using the pulse-per-second signal from the GPS receiver. The GPS timing code can provide the the precise time for sferic detection to within 200 nanoseconds. The ADC has the sample rate of 48 kS/s and 16 bit precision. We use the SpectrumLab v2.77b22 to record the sound files with extension "wav". The time of clock on PC is synchronized by a GPS receiver, thus, the clock is corrected with UTC.

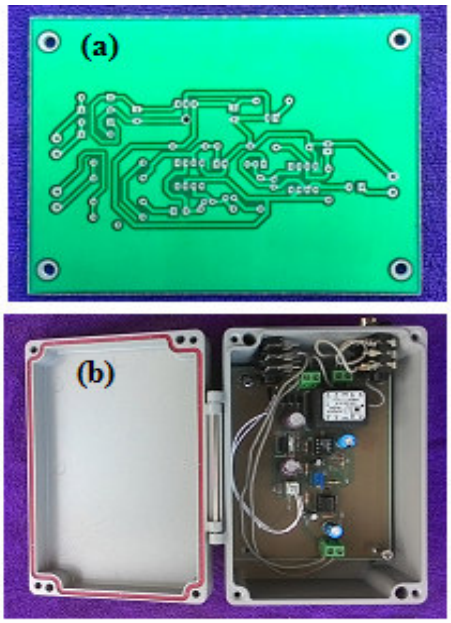

Figure 4. a) Printed circuit board, b) printed circuit board assembled with electronic components in a metal box.

2.3. Frequency response

A generator is used to provide the input of pre-amplifier with the sine-shaped signal of 34 mV and the frequency varying from 100 Hz to 100 kHz. The oscilloscope is used to record the output signal. We adjust the variable resistor (VR) to receive the undistorted signal and measure the output voltages, then calculate the gain of the pre-amplifier in dB.

The effects of high-pass filter and low-pass filter can be seen by the solid line in Figure 5. The 3 dB points appear at ~340 Hz on the low side and at ~34 kHz on the high side, hence the bandwidth is 33.6 kHz. The flat frequency response is in the frequency range of 1 – 20 kHz. If the high-pass filter is not used, the noise sources of AC power will be fed and amplified by receiving system. The high-pass filter keeps the frequency response low at frequencies below 340 Hz to remove the hum noise from power lines. It can be concluded that the pre-amplifier can record the broadband signals radiated by lightning discharges.

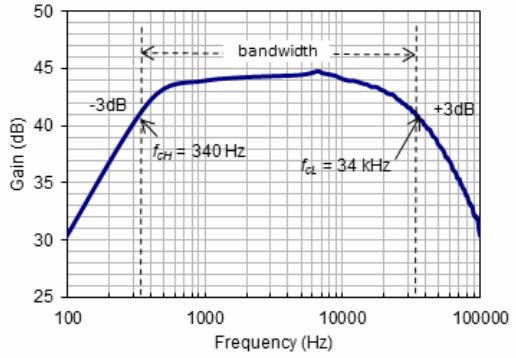

Figure. 5. The frequency response of pre-amplifier.

III. EXPERIMENTAL RESULTS

SpectrumLab is adjusted to the sample rate of 44.1 kS/s, and FFT input size of 512 to record the broadband data. The sound files are recorded every fifteen minute from 12:00 to 22:00 UT (local time, LT = UT + 7 h). The two-minute-length of each file is analyzed. The cut-off frequency is obtained from the tweeks at Tay Nguyen University, a low-latitude site (Geog. 12.65° N, 108.02° E) on ten quiet days of May and June, 2013. Figure 6 shows the spectrogram with the frequency under 22 kHz at the night on 21 February, 2014. The vertical lines are the pulses of sferics which expend all frequencies. The horizontal lines show the VLF signals of some transmitters, i.e. NWC/19.8 kHz from Australia, and VTX2/16.2 kHz from India.

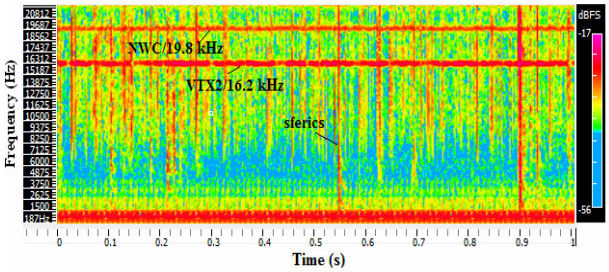

Figure 6. Spectrogram shows many sferics on 21 February, 2014.

Table 1 presents a total of 9170 tweeks with m = 1 - 8 observed during May and June, 2013. The tweeks with m = 2 – 5 often occurred. Tweeks with m = 4 are most often (25.49 %), but the higher harmonic tweeks (m = 7 - 8) occurred rarely, especially tweeks with m = 8.

Figure 7 shows the tweeks as the “hooks" appeared on spectrogram. Some tweeks with mode number m = 2, 3 (Figure 7a) and 8 (Figure 7a) clearly occurred.

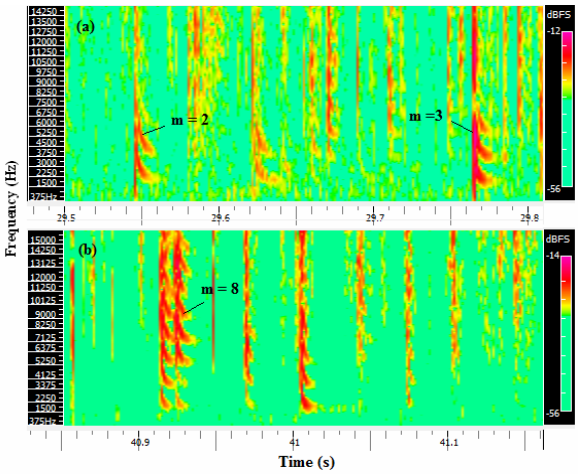

Figure 7. Example of spectrograms showing the tweek events on 15 May 2013 at 1:30 LT (a), and 2:30 LT(b).

Table 1. Tweek occurrence observed during May and June, 2013

	Harmonics								Total
Mode number	1	2	3	4	5	6	7	8	
occurrence	149	1543	2337	2195	1593	811	421	121	9170
%Count	1.62	16.83	25.49	23.94	17.37	8.84	4.59	1.32	100.00

The reflection height of EIWG and electron density of lower ionosphere is calculated by equations [16-18],

$$h = \frac{cm}{2 f_{cm}} \quad (5)$$

$$N_e = 1.24 \times 10^{-8} f_c f_H \quad (6)$$

The propagation distance of tweek sferics is obtained by [19]:

$$d = \frac{|t_2 - t_1|(v_{gf1} \times v_{gf2})}{v_{gf1} - v_{gf2}} \quad (7)$$

where, $t_2 - t_1$ is the difference in arrival times of the two frequencies, f_2 and f_1, close to the tweeks of any mode, and v_{gf1} and v_{gf2} are the corresponding group velocities of the radio waves centered at frequencies f_1 and f_2.

where, c is the velocity of light in free space, m is the order mode number, f_{cm} is cut-off frequency and f_H is the electron gyro-frequency. We consider tweeks occurred in the low-latitude and equatorial regions, so we choose $f_H = 1.3$ MHz [6].

Table.2. The mode number (m), the fundamental frequency (f_{cm}/m), reflection height (h), propagation distance from lightning discharges to the receiver (d), and electron density (N_e) obtained from tweeks on Figure 7.

Spectro -gram	m	f_{cm}/m (Hz)	h (km)	d (km)	N_e (cm^{-3})
Figure 7.a	1	2135	70.25	15099	34.45
	2	1922	78.06	7516	62.01
	1	1876	79.95	7377	30.27
	2	1792	83.69	5056	57.83
	3	1747	85.86	4154	84.56
Figure 7.b	1	1931	77.70	3599	31.15
	2	1882	79.70	2933	60.72
	3	1847	81.20	2730	89.40
	4	1844	81.36	2972	118.98
	5	1853	80.96	1602	149.45
	6	1822	82.34	1301	176.34
	7	1792	83.72	1716	202.34
	8	1818	82.52	917	234.60

Table 2 shows that the reflection height (h) varies from 70.25 - 85.86 km, the electron density (N_e) changes in the range of 30.27 - 234.60 cm^{-3}, and the fundamental frequency (f_{cm}/m) varies within 1.8 - 2.14 kHz. The propagation distance (d) varies from 917 - 15099 km.

Analyzing 9170 tweeks during May and June, 2013 and removing tweeks with $d > 6000$ km, it is seen that the mean reflection height increases from 80.74 – 85.53 km with standard deviation SD_h = ± 3.65 to ± 1.18 km as mode number increases from 1 – 8, and the mean fundamental frequency reduces from 1.87 – 1.75 kHz with SD_f = ± 90 to ± 24 Hz (see Table 3 and Figure 8). The mean value of electron density increases from 30 - 227 cm^{-3} (SD_e = ± 4.24 to ± 1.4 cm^{-3}), which corresponds to m = 1 - 8. Shvets and Hayakawa (1998) observed tweeks with m = 1 - 8 and calculated the electron density to vary from 28 – 224 cm^{-3}. Our result in electron density variation has a good comparison with that reported by Shvets and Hayakawa [20].

Table 3. The mode number (m), mean reflection height (h_m), mean electron density (N_m), the mean fundamental frequency (f_m). SD_h, SD_e, SD_f indicate the standard deviation of h_m, N_m, and f_m, respectively.

m	h_m (km)	SD_h (km)	N_m (cm^{-3})	SD_e (cm^{-3})	f_m (Hz)	SD_f (Hz)
1	80.74	3.65	30.22	1.44	1872	90
2	83.80	1.96	57.95	1.40	1795	42
3	84.16	1.41	86.43	1.45	1786	29
4	84.42	1.24	114.79	1.58	1780	25
5	84.97	1.18	142.65	1.86	1767	24
6	85.09	1.30	170.22	2.64	1764	26
7	85.00	1.22	199.22	2.17	1766	25
8	85.53	1.59	226.66	4.24	1754	33

Observing the tweeks in the period of September 2003 – July 2004 at Suva, Kumar et al. (2008) found that the fundamental frequency slightly reduces from 1.84 - 1.72 kHz corresponding to the harmonics of 1 – 6. The tweeks can be reflected at the altitudes where the plasma frequency equals the individual cut-off frequency of each mode, hence the waves with the higher harmonics can be reflected at the higher altitude due to the plasma frequency is higher [20].

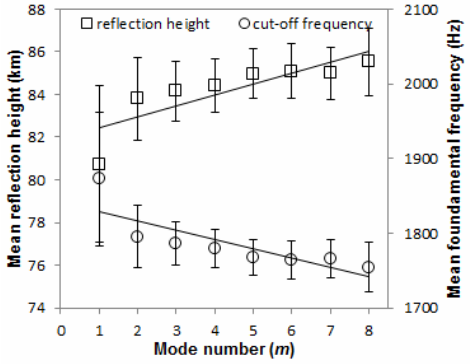

Figure 8. Variation of reflection height (squares, left hand side) and mean fundamental frequency (circles, right hand side) of tweeks with mode number. The error bars indicate a standard deviation in the estimated height and fundamental frequency.

To estimate the errors of our results, we calculated the standard deviations of mean f_{cm}/m and then used equations (5) and (6) to estimate the errors of mean h and N_e. The reading errors of mean f_{cm}/m , mean h, and mean N_e are about ± 37 Hz, ± 1.7 km, and ± 0.6 cm^{-3}, respectively. Ohya et al. (2003) found that the errors of mean f_{cm}/m were about ± 38 Hz, which corresponds to ± 1.9 km for the reflection height, and errors of < 1 cm^{-3} for the electron density [18]. Our reading errors are lower than those reported by these authors. In addition, the frequency band which our remote sensing can record is wider than that of Inspire VR-3 receiver. This receiver can detect sferis with frequency range of 10 kHz . It means that we have an opportunity to record higher harmonic tweeks.

IV. CONCLUSIONS

Our ELF/VLF remote sensing includes a loop antenna, a pre-amplifier, a sound card, a PC with Spectrum Lab and a GPS receiver. The antenna and pre-amplifier of remote sensing are designed. Therefore, this system has low cost. We designed the square loop antenna with 14 turns of 18 AWG copper wire and the base of 1 m. It has an extremely high sensitivity. The pre-amplifier designed has the bandwidth of 33.6 kHz and has the flat frequency response of 1 – 20 kHz. The ELF/VLF remote sensing can record tweek sferics generated by lightning discharges. Using cut-off frequency obtained from tweeks, we can estimate the parameters of the nighttime D-region ionosphere. Observing tweeks with $m = 1 – 8$ during May and June 2013 at Tay Nguyen university (Geog. 12.65^o N, 108.02^o E), results reveal that the mean fundamental frequency varies within 1.75 – 1.87 kHz, which corresponds to the reading error of ± 37 Hz. The ELF/VLF remote sensing designed can give not only the confident data for studying the lower ionosphere, but also the experimental module for students at universities in Vietnam.

ACKNOWLEDGEMENT

We would like to thank Paul Nicholson (www.vlf.it) for giving useful ideas and helps.

REFERENCES

[1] J. K. Hargreaves, *The Solar – Terrestrial environment*, Cambridge Univesity Press, 1992.
[2] G. T. Wood, *Geo-locaction of individual lightning discharges using impulsive VLF electromagnetic waveforms*, Ph.D. Thesis, Department of Electrical Engineering, Stanford University, 2004.
[3] S. C. Reising, U. S. Inan, and T. F. Bell, "ELF sferic energy as a proxy indicator for sprite occurrence", *Geophysical Research Letters*, Vol. 26, 987-990, 1999.
[4] Budden, K. G (1962), "The influence of the earth's magnetic field on radio propagation of waveguide modes", *Proceedings of the Royal Society A*, 265, pp.538, 1962.
[5] R. A. Helliwell, *Whistlers and Related Ionospheric Phenomena*, Stanford University Press, 1965.
[6] S. Saini, and A. K. Gwal, "Study of ELF – VLF Emisson and Tweek Atmospherics Observed at "Maitri"", *Ministry of Earth Sciences, Techical Publication*, No. 22, 135 - 155, 2005.
[7] S. Kumar, A. Kishore, and V. Ramachandran, "Higher harmonic tweek sferics observed at low latitude: estimation of VLF reflection heights and tweek propagation distance", *Ann. Geophys*, Vol. 26, 1451-1459, 2008.
[8] A. K. Maurya, R. Singh, B. Veenadhari, P. Pant, and A. K. Singh, "Application of lightning discharge generated radio atmospherics/tweeks in lower ionospheric plasma diagnostics*", J. Phys.: Conf. Ser.* Vol. 208, 012061, 2010.
[9] A. K. Maurya, B. Veenadhari, R. Singh, S. Kumar, M. B. Cohen, R. Selvakumaran, S. Gokani, P. Pant, A. K. Singh, U. S. Inan, "Nighttime D region electron density measurements from ELF-VLF tweek radio atmospherics recorded at low latitudes", *Journal of Geophysical Research,* Vol. 117, A11308, 2012.
[10] M. Marbouti, M. Khakian Ghomi, M. R. Salmanpour, K. Ghanbari, B. Nahavandi, L. M. Tan, "Designing and constructing a VLF radio telescope with an external filter to receive the Sudden Ionospheric Disturbances (SID) in Iran", *Proceeding of 10th International Conference on "Technical and Physical Problems of Electrical Engineering*, 7-8 September 2014, Institute of Physics, Azerbaijan National Academy of Sciences Baku, Azerbaijan.
[11] Dolea, P, V . Dascal, T. Palade, O. Cristea, "Low-cost prototype equipment for VLF radio wave monitoring", *ACT Technica Napocensis – Electronics and Telecommunications*, Vol. 53, No. 1, 47-51, 2012.
[12] W. D. Reeve, *Application of the UKRAA Very Low Frequency Receiver System*, British Astronomy Association (BAA), Radio Astronomy Group (RAG), 2010. [Online]. Available: http://www.reeve.com/Documents/LF-VLF/Reeve_SARA%20WestConf%20VLF%20Paper_Upd.pdf.
[13] E. W. Paschal, *The design of broad-band VLF receivers with air-core loop antenna*, Stanford University, 1988. [Online]. Available: http://traktoria.org/files/radio/antenna/VLF/.
[14] S. K. Harriman, E. W. Paschal, U. S. Inan, "Magnetic Sensor Design for Femtotesla Low-Frequency Signals", *IEEE transactions on Geoscience and Remote sensing*, Vol. 48, No. 1, :396-402, 2010.
[15] C. Kitchin, "Avoiding Op Amp instability problems in single-supply applications", *Analog Dialogue*, vol. 35, No. 2, 2001. [Online]. Available: http://www.analog.com/library/analogDialogue/archives/35-02/avoiding/avoiding.pdf
[16] K. G. Budden, *The Wave-Guide Mode Theory of Wave Propagation*, Logos Press, London, 1961.
[17] M. Yamashita, "Propagation of tweek atmospherics", *J. Atmos. Terr. Phys.* Vol. 40, 151-156, 1978.
[18] H. Ohya, M. Nishino, Y. Murayama, and K. Igarashi, "Equivalent electron density at reflection heights of tweek atmospherics in the low- middle latitude D-region ionosphere", *Earth Planets Space*, Vol. 55, 627–635, 2003.
[19] R. Prasad, "Effects of land and sea parameters on the dispersion of tweek atmospherics*", J. Atmos. Terr. Phys.*, Vol. 43, 1271–1277 , 1981.
[20] A. V. Shvets and M. Hayakawa, "Polarization effects for tweek propagation", *J. Atmos. Terr. Phys.,* Vol. 60, 461 – 469, 1998.